Monitoring Growth of Surfactant-Free Nanodroplets Dispersed in Water by Single-Droplet Detection

Toshio Sakai,[†,‡] Yoshihiro Takeda,[§] Fumitaka Mafuné,[||] Masahiko Abe,[†] and Tamotsu Kondow*[,||]

Faculty of Science and Technology, Tokyo University of Science, 2641 Yamazaki, Noda, Chiba 278-8510, Japan, East Tokyo Laboratory, Genesis Research Institute, Inc., 717-86 Futamata, Ichikawa, Chiba 272-0001, Japan, and Cluster Research Laboratory, Toyota Technological Institute, 717−86 Futamata, Ichikawa, Chiba 272-0001, Japan

Received: August 15, 2002; In Final Form: December 18, 2002

Nanodroplets of *n*-decane (50−300 nm in diameter) containing Coumarin 540 were dispersed ultrasonically in water under a surfactant-free condition, and their growth process was observed by a method of a single-droplet detection in which fluorescence-bunching signals from individual nanodroplets passing through the focal volume of an excitation laser were collected and detected in a confocal fluorescence microscope. The volume of the nanodroplets determined from the fluorescence-bunching signals increased stepwise with time; time regimes of gradual and rapid increases were attributed to Ostwald ripening and coalescence, respectively. The alternative manifestation of the two growth processes is consistent with an observed oscillatory behavior of the surface charge density of the nanodroplets.

Introduction

Destabilization of an emulsion proceeds mainly via Ostwald ripening[1−7] (isothermal distillation) in which larger droplets grow at the expense of smaller ones by diffusion of molecules contained in the droplets through the continuous phase by taking advantage of differences in their chemical potentials or via coalescence,[8−14] that is, fusion of several constituent droplets into a single larger droplet. Theoretically, Ostwald ripening and coalescence are described by the Lifshitz−Slyozov−Wagner (LSW) theory[6,7] and by the Derjaguin−Landau−Verwey−Overbeek (DLVO) theory,[8,9] respectively. Experimentally, however, it is still a difficult task to establish the mechanism of droplet growth in emulsions because of complicate functioning of emulsion components such as continuous and dispersed media, surfactant, cosurfactant, and so forth.

It has been reported that in hydrocarbon oil-in-water emulsions stabilized by surfactants the growth mechanism (Ostwald ripening vs coalescence) varies characteristically with the chain length of the hydrocarbon molecule which constitutes the oil.[2,3,15] A similar tendency has also been observed in surfactant-free emulsion systems.[16−20] This tendency is particularly evident in emulsions of aliphatic linear chain hydrocarbons. For instance, droplets of hydrocarbons whose chain lengths are longer than *n*-decane (e.g., *n*-dodecane, *n*-tetradecane, and *n*-hexadecane) grow according to the Ostwald ripening scheme in a surfactant-free condition.[20] The growth rates of the droplets are measured to be about 10^{-26}−10^{-27} m^3 s^{-1}, which are consistent with the rates calculated by LSW theory.[20]

On the other hand, droplets of hydrocarbons with shorter chains such as *n*-hexane and *n*-octane have been reported to grow much more rapidly by coalescence; it takes about 1 h to grow from droplets with diameters of several hundred nanometers to those with diameters of several micrometers with the rates of $\sim 10^{-21}$ m^3 s^{-1}.[20] The growth rates are comparable with the rate of coalescence occurring at every collision of the droplets (r_{ECC}).

In the growth of *n*-decane droplets, the growth mechanism is not simply explained by the Ostwald ripening and by coalescence. In an *n*-decane-in-water emulsion stabilized by sodium dodecyl sulfate (SDS), the *n*-decane droplets are reported to grow according to the Ostwald ripening scheme.[2,3] The rate of the Ostwald ripening is comparable to the rate calculated by LSW theory; the experimental value of 3.5×10^{-25} m^3 s^{-1} versus the calculated value of 1.8×10^{-25} m^3 s^{-1}.[2,3] On the other hand, the growth rate of surfactant-free *n*-decane droplets is measured to be 12×10^{-25} m^3 s^{-1} by the dynamic light-scattering method, which is about 7 times as large as the rate calculated by LSW theory.[20] This finding indicates that the growth of the surfactant-free *n*-decane droplets involves coalescence in addition to Ostwald ripening which always proceeds in any emulsions.

We have developed a method of observing a single droplet of *n*-decane labeled with fluorescing dye molecules suspended in water by detecting the fluorescence spike from the droplet using a confocal fluorescence microscope. The volume of a droplet is evaluated by the intensity of the fluorescent spike signal from the dye molecules in the droplet and the number of individual droplets passing through the focal volume of the microscope per unit time is given by the frequency of the fluorescent spikes. This method is applicable to observe a growth process of surfactant-free *n*-decane droplets suspended in water because the dye molecules are measured to diffuse much more rapidly[21] than the droplets grow in water as predicted by LSW and DLVO theories on Ostwald ripening and coalescence.[20] In other words, the dye molecules are distributed so rapidly among all the droplets in water that the droplets are always shared with an equilibrium amount of the dye molecules, and hence the

* To whom correspondence should be addressed. Phone:+81-47-320-5911; fax: +81-47-327-8031; e-mail: kondow@clusterlab.jp.
† Tokyo University of Science.
‡ Present address: East Tokyo Laboratory, Genesis Research Institute, Inc., 717-86 Futamata, Ichikawa, Chiba 272-0001, Japan.
§ Genesis Research Institute, Inc.
|| Toyota Technological Institute.

10.1021/jp021887j CCC: $25.00
Published on Web 03/07/2003

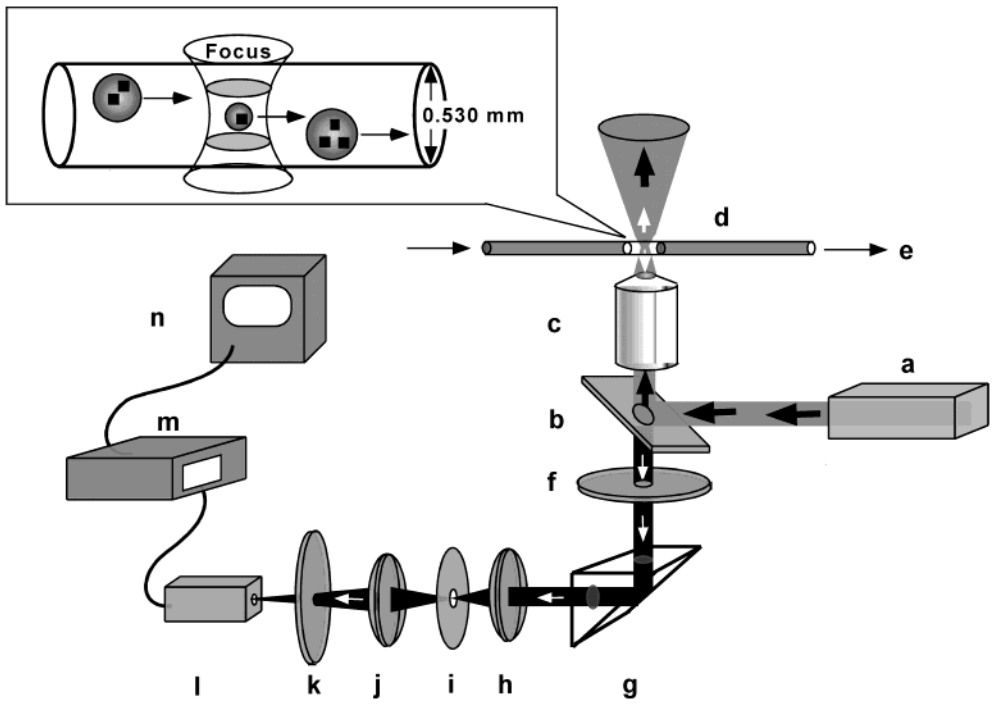

Figure 1. Experimental setup consisting of (a) argon ion laser, (b) dichroic mirror (DM505), (c) objective lens, (d) capillary, (e) sample, (f) high-pass filter (>515 nm), (g) prism, (h) convex lens, (i) pinhole (20 μm in diameter), (j) convex lens, (k) band-pass filter (520−550 nm), (l) avalanshe photodiode, (m) multichannel counter, and (n) computer.

intensity and the frequency of the fluorescence spike signals provide authentic information on the droplet growth. This method has an advantage over the light-scattering method that the number of the droplets per unit time can be measured directly and easily. In the present study, this single-droplet detection method was applied to the study on the growth of surfactant-free *n*-decane droplets dispersed in pure water.

Experimental Section

Materials and Sample Preparation. Emulsions were prepared by mixing *n*-decane (GR grade, Tokyo Kasei Co., Ltd.) dissolved with 1×10^{-5} mol L^{-1} of Coumarin 540 (C540; laser grade, Exciton, Inc.) with deionized water having the electric conductivity of 5.58 μS cm^{-1} (Ohtsuka Pharmacy Co., Ltd.) by using an ultrasonic cleaner (FU-10C, 60 W, 28 kHz, Tokyo Garasu Kikai Co., Ltd.). The concentration of the emulsion droplets in the water was 5×10^{-4} mol L^{-1} and hence that of C540 in the emulsion turns out to be 1×10^{-9} mol L^{-1}. Emulsion droplets freshly prepared were measured to have an average diameter of ∼50 nm by use of the dynamic light-scattering method.

Single-Droplet Detection. The method described below is essentially the same as that reported previously.[21] Fluorescence emitting from C540 molecules in individual droplets was detected by an avalanche photodiode in a confocal fluorescence microscope (IX70,OLYMPUS) (see Figure 1). A sample solution maintained at an ambient temperature of 23 ± 1 °C was allowed to flow through a glass capillary with the inner diameter of 0.530 mm at a flow rate of $\sim 1.06 \times 10^{-3}$ L min^{-1} by a pump, which was optimized as described in the following section. The lowest limit of the flow rate was set in such a procedure that droplets pass through the capillary rapidly enough not to establish the adsorption equilibrium with the inner capillary surface. The capillary tube was placed right above the objective lens (UplanApo 100 × Oil I, OLYMPUS). An argon ion laser (BeamLok 2060-7S; Spectra-Physics, Co.) was used to excite C540 molecules in a single droplet at the wavelength of 476.5 nm. Fluorescence signals from the droplet passing through the focal volume of the laser beam were collected by the same objective lens employed for focusing the excitation laser and were detected by an avalanche photodiode with a quantum efficiency of ∼70%. Rayleigh and Raman scattering lights from solvent molecules were removed prior to the detection by using a combination of high-pass (>515 nm) and band-pass filters (520−550 nm). The fluorescence signals were processed and registered with a multichannel counter (Stanford Research Systems, SR430), where the gate time of the multichannel counter was set to 1.3 ms. In the present confocal configuration, a pinhole of a 20-μm diameter was located at the conjugated position in front of the photodiode. The fluorescence was so focused at the pinhole that the fluorescence signals from the focal volume was maximized and otherwise minimized by being defocused at the pinhole. The focal volume has the depth of 1 μm and the diameter of 0.8 μm with the volume of 5×10^{-16} L.

Zeta Potential Measurement. A ζ-potential on the surfaces of *n*-decane droplets in a *n*-decane-in-water emulsion was measured by the laser Doppler method (heterodyne method) (NICOMP 380 ZLS, Particle Sizing System Co.). The electrophoretic mobility and the ζ-potential of the droplets moving in an electric field (typically 5.0 V cm^{-1}) were obtained from the Doppler shift of a 535-nm laser having a 10 mW power (solid-state laser pumped by a diode laser) scattered by the droplets at the scattering angle of 19.8°.

Data Analysis. *Condition of Single-Droplet Detection.* The avalanche photodiode of the confocal microscope produces the output of a spikelike fluorescence signal (bunching signal) every time when a droplet containing C540 dye molecules is traveling across its focal volume (see Figure 2). The initial droplet concentration is obtained from the volume of *n*-decane mixed initially with water and the distribution of the diameters of freshly prepared droplets. At a droplet concentration less than

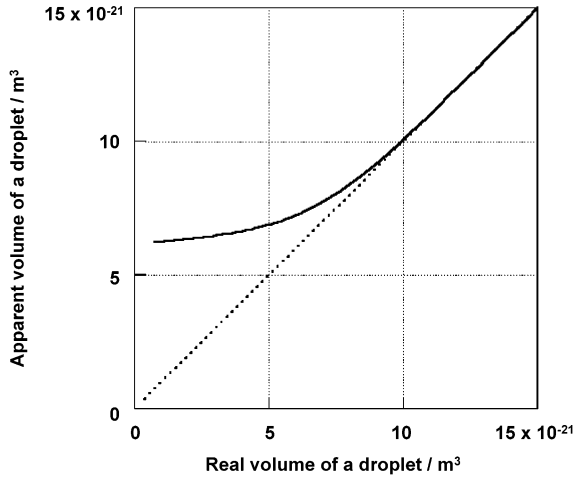

Figure 2. Apparent volume of one droplet obtained from the average intensity (I_{measd}) measured as a function of the real volume of the droplet obtained from the dye concentration in *n*-decane.

10^{-9} mol L^{-1}, the single-droplet detection is achieved because the probability for finding more than two droplets in the focal volume is calculated to be negligibly small (see eq 1 in ref 21).

Under laser irradiation at 476.5 nm, a C540 molecule in a single droplet emits $\sim 10^8$ photons s^{-1} in the wavelength range of 480−550 nm by repeating absorption and emission cycles. In this single-droplet detection experiment, a single droplet containing C540 molecules flows through the focal volume and emits photons. Each C540 molecule emits photons independently, and hence the intensity of the bunching fluorescence signal should be proportional to the number of the C540 molecules in the droplet. An average residence time of the droplet in the focal volume is ~ 10 μs at a flow velocity of $\sim 1.06 \times 10^{-3}$ L min^{-1} in the glass capillary. Therefore, each C540 dye molecule during its traversing across the focal volume emits photons which are detected as photon counts less than 1000 and typically 2−3 by a photon detector with a quantum efficiency of ~1%. Fluorescence from C540 molecules in water must be negligible because practically the dye molecules are not dissolved in water. According to our previous study,[21] the dye molecules in a droplet transfer so rapidly to another droplet that the dye molecules are evenly distributed among all the droplets within a minute after being dispersed supersonically; in other words, the rate of the dye molecule transfer is much faster than the growth rate of the droplets.

Estimation of Volume and Number of Droplets. The growth processes of surfactant-free *n*-decane droplets in water were investigated by measuring the volumes of the individual droplets and their number per unit time (proportional to the number density) passing through the focal volume, which were determined from the intensity of the corresponding fluorescence-bunching signal and the number of the bunching signals per unit time, respectively. Actually, the average diameter of the droplets at the beginning of regime d (see the definition of regime d in Results) was measured by the dynamic light-scattering method and then was compared with the intensity of the bunching signals from the droplets obtained by averaging for the time interval of 1.3 s. In deriving the volume of a single droplet from the corresponding bunching signal, it is presumed that the dye molecules are randomly distributed among different droplets, and a different droplet takes a different trajectory in the focal volume of the microscope, as described below.

The intensity of a fluorescence-bunching signal depends on the number of dye molecules in the corresponding single droplet and a trajectory that the droplet passes through the focal volume of the microscope. In a random distribution of the dye molecules among all the droplets, the probability of finding a droplet with a given volume which contains *m* molecules of the dye is given by a Poisson's distribution function, $P_\alpha(m)$, where α divided by the volume of the droplet gives a dye concentration in *n*-decane. To detect the droplet, one admits it passing through the focal volume and measures the intensity of its fluorescence-bunching signal by the detector. Suppose that the droplet takes such a trajectory through the focal volume that the intensity of the corresponding bunching signal has a value between I' and $I' + dI'$. It is easily shown that the intensity of the bunching signal, $I(m)$, is proportional to $P_\alpha(m)\int f_m(I')I'dI'$, where $f_m(I')$ represents a normalized distribution function of the intensity, I', by taking into consideration the fact that every droplet passing through the focal volume does not always take the same trajectory:

$$I(m) \propto P_\alpha(m)\int_0^\infty f_m(I')I'dI' \tag{1}$$

$$\int_0^\infty f_m(I')dI' = 1 \tag{2}$$

The integral, $\int_0^\infty f_m(I')I'dI'$, can be approximated by the time-averaged intensity which is proportional to the number of the dye molecules, *m*, in the droplet. It turns out that the intensity of the fluorescence-bunching signal from the droplet containing *m* dye molecules is still proportional to Poisson's distribution function, $P_\alpha(m)$, even after one takes into account the effect that every droplet does not always take the identical trajectory.

In the present experimental condition, there is a minimum detectable intensity (I_{th}) below which the bunching signal is too weak to be measured reliably. In a low dye concentration, the average intensity (I_{measd}) measured from the bunching signals could differ from the real average intensity (I_a) of the bunching signals given by the condition of $I_{th}=0$ because one may miss detecting smaller droplets producing fluorescence-bunching signals whose intensities are less than the minimum detectable intensity. Then the following relation is obtained:

$$I_{measd} \propto \frac{\alpha - e^{-\alpha}\sum_{m=0}^{m_{th}-1} m\frac{\alpha^m}{m!}}{1 - e^{-\alpha}\sum_{m=0}^{m_{th}-1}\frac{\alpha^m}{m!}} \tag{3}$$

where m_{th} multiplied by the overall detection efficiency gives the minimum detectable intensity, I_{th}. The proportional constant of eq 3 was obtained by using a droplet having the diameter of ~300 nm in such a manner that I_{measd} was obtained and compared with the average number of the dye molecules in the droplet evaluated from the dye concentration in *n*-decane. In the present experimental condition, the minimum detectable intensity (I_{th}) was obtained to be ~17 counts 1.3 s^{-1}.

Figure 2 shows the apparent volume of a droplet obtained from average intensities (I_{measd}) (see eq 3) as a function of the real volume of the droplet obtained from the dye concentration in *n*-decane. As shown in Figure 2, the apparent volume agrees with the real volume in the region larger than $\sim 10 \times 10^{-21}$ m^3, while it tends to level off below $\sim 10 \times 10^{-21}$ m^3 with decrease in the real volume. In other words, it is difficult to discriminate droplets having different volumes by this method in this smaller volume region. It is concluded that the smallest volume that can be measured with the systematic error of less than 10% turns out to be $\sim 7 \times 10^{-21}$ m^3 (~240 nm in diameter).

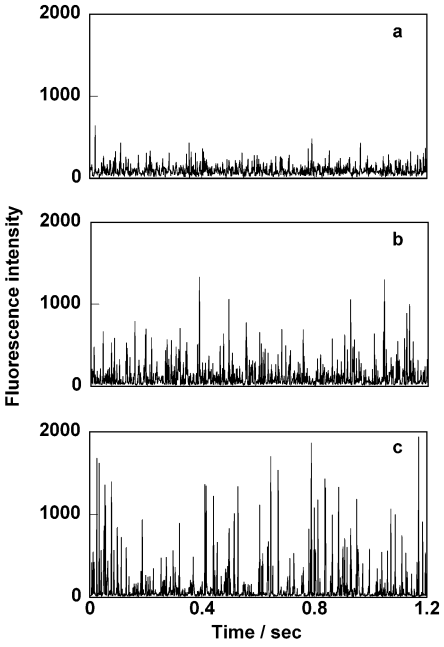

Figure 3. Fluorescence signals from individual *n*-decane droplets labeled with C540 dye molecules dispersed in water at the elapsed times of 3 min (panel a), 60 min (panel b), and 180 min (panel c) after preparation of the emulsion.

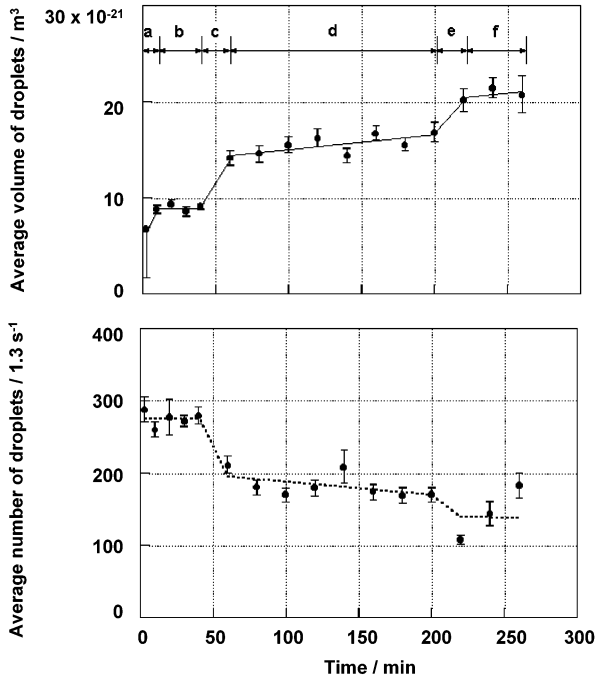

Figure 4. Average volume (upper) and number (lower) of *n*-decane droplets as a function of the time lapsed after the preparation of the *n*-decane-in-water emulsion. In regimes a, c, and e, the average volume increases rapidly, while in regimes b, d, and f, it increases gradually.

Results

Figure 3 shows time dependences of spikelike fluorescence signals (bunching signals) produced by individual *n*-decane droplets containing C540 dye molecules dispersed in pure water at three different elapsed times after preparation of the emulsion by an ultrasonic cleaner. Panels a, b, and c show the time dependences of the bunching signals measured at 3, 60, and 180 min after preparation of the *n*-decane-in-water emulsion, respectively. Low but dense bunching signals are observed at 3 min after the preparation (see panel a), while the heights of the signals increase but the frequencies decrease with the elapsed time.

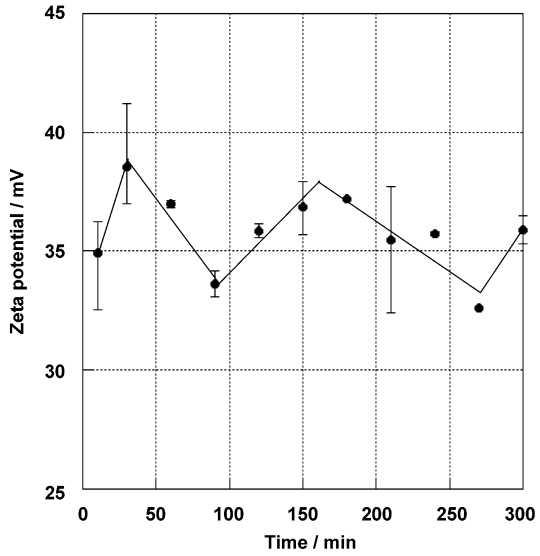

Figure 5. Change of the ζ-potential of the *n*-decane droplets with the elapsed time. In general, the ζ-potential increases in a regime where coalescence takes place while decreases in a regime where Ostwald ripening is the dominant growth process.

Figure 4 shows the average volume and the average number of the droplets as a function of the elapsed time after the preparation (see the section of Data Analysis for the determination of these values). As shown in the upper panel of Figure 4, the average volume increases stepwise with the elapsed time: the first rapid increase up to the elapsed time of 10 min (regime a) followed by the first gradual increase from 10 to 40 min (regime b), the second rapid increase (regime c) followed by the second gradual increase from 60 to 200 min (regime d), and the third rapid increase (regime e) followed by the third gradual increase after 220 min (regime f). It is calculated that the growth rates of the droplets in the regimes of the rapid increase (regimes a, c, and e) are in the range of 10^{-24} m^3 s^{-1} while those of the regimes of the gradual increase (regimes b, d, and f) are in the range of 10^{-25} m^3 s^{-1}. As shown in the lower panel of Figure 4, the number of the droplets per 1.3 s decreases stepwise with the elapsed time correspondingly to the stepwise increase of the average volume of the droplets. The number of the droplets per 1.3 s is proportional to the number density.

Figure 5 shows the ζ-potential of the *n*-decane droplets dispersed in water as a function of the elapsed time after the preparation of the droplets. There is a general trend that the ζ-potential (−35 mV for fresh droplets) increases with the elapsed time in the rapid increase regimes of the droplets but decreases in the gradual increase regimes of them.

Discussion

Gradual Growth by Ostwald Ripening Versus Rapid Growth by Coalescence. Lifshitz, Slyozov, and Wagner have developed LSW theory which describes Ostwald ripening of oil droplets in an oil-in-water emulsion.[6,7] The rate of the Ostwald ripening (ω) is expressed as

$$\omega = \frac{da^3}{dt} = \frac{8Dc_\infty \gamma V_m^{\ 2}}{9RT}, \qquad (4)$$

where a is the mean radius (m) of the oil droplets, t is time (s),

γ is the interfacial tension at an oil−water interface (N m^{-1}), D is the diffusion coefficient of the oil molecule through water, c_∞ is the solubility of the oil in water (mol m^{-3}), V_m is the molar volume of the oil (m^3 mol^{-1}), R is the gas constant (J mol^{-1}), and T is an absolute temperature (K) (T represents the room temperature in this paper if otherwise noted). In an *n*-decane-in-water emulsion, the Ostwald ripening rate is calculated by LSW theory to be $\sim 1.8 \times 10^{-25}$ m^3 s^{-1},[3,20] while the experimental rates were obtained to be 1.6×10^{-26}, 2.6×10^{-25}, and 2.4×10^{-25} m^3 s^{-1} for regimes b, d, and f, respectively. The reasonable agreement of the experimental rates for regimes b, d, and f with the calculated Ostwald ripening rate leads us to conclude that the *n*-decane droplets grow by Ostwald ripening in the gradual growth regimes (regimes b, d, and f).

On the other hand, the measured growth rates in regimes a, c, and e are much larger than the theoretical Ostwald ripening rate. This finding indicates that the other growth mechanism, that is, coalescence, operates in these regimes. Therefore, the rates of coalescence (r_{COA}) in regimes a, c, and e are derived by subtraction of the rate of the Ostwald ripening (the calculated or the experimental rates in regimes b, d, and f) from the experimental rates in regimes a, c, and e.

If *n*-decane droplets in water coalesce by every collision of the droplets, the growth rate (r_{ECC}) is calculated to be $\sim 1.8 \times 10^{-21}$ m^3 s^{-1} at 5×10^{-4} mol L^{-1} of the *n*-decane concentration in water by using the Smoluchowski equation[22]

$$r_{ECC} = \frac{da^3}{dt} = \frac{4kT}{3\eta} N v \tag{5}$$

where a, t, k, T, η, N, and v are the mean radius (m) of the *n*-decane droplets, time (s), the Boltzmann constant (J K^{-1}), a temperature (K), the viscosity of water (Pa s), the number density of the *n*-decane droplets (m^{-3}), and the volume of one oil droplet (m^3), respectively. In reality, the growth rate thus calculated is much larger than the experimental rates of 5.0×10^{-24}, 4.2×10^{-24}, and 2.8×10^{-24} m^3 s^{-1} for regimes a, c, and e, respectively, mainly because colliding droplets do not always coalesce at every collision. For the droplets to fuse, the colliding system of the droplets should overcome a potential energy barrier on the interaction potential energy constructed from attractive and repulsive potential energies of the system. The potential energy barrier (V_{max}) appears when the repulsive potential energy exceeds the attractive potential energy. By use of this interaction potential energy, Reerink and Overbeek derive a stability ratio (W) in terms of V_{max}/kT as[23]

$$W \cong \frac{1}{2\kappa a} \exp\left(\frac{V_{max}}{kT}\right) = r_{ECC}/r_{COA} \tag{6}$$

where $1/W$ is the probability that coalescence occurs by one collision event or the rate constant of the coalescence, κ is the Debye−Hückel parameter, a is a droplet radius, k is the Boltzmann constant, and r_{COA} and r_{ECC} represent the rates of coalescence with and without the potential energy barrier, respectively. The ratio of r_{ECC} ($\sim 1.8 \times 10^{-21}$ m^3 s^{-1}) to r_{COA} gives the coalescence probability ($1/W$). Figure 6 shows the coalescence probability ($1/W$) thus obtained as a function of the elapsed time. In regimes a, c, and e, where the coalescence take places, the probability is sizable and otherwise almost zero.

Relation of Stepwise Growth with Surface Charge Density. In the present *n*-decane-in-water emulsion, the droplets of *n*-decane are negatively charged and the ζ-potential of the droplets changes with the elapsed time characteristically (see Figure 5). The negative charge originates from OH^- attached on the droplets.[24,25] It is reasonable to consider that the characteristic change of the surface charge density is closely related to the stepwise growth; Ostwald ripening and coalescence occur alternatively in the growth of the droplets.

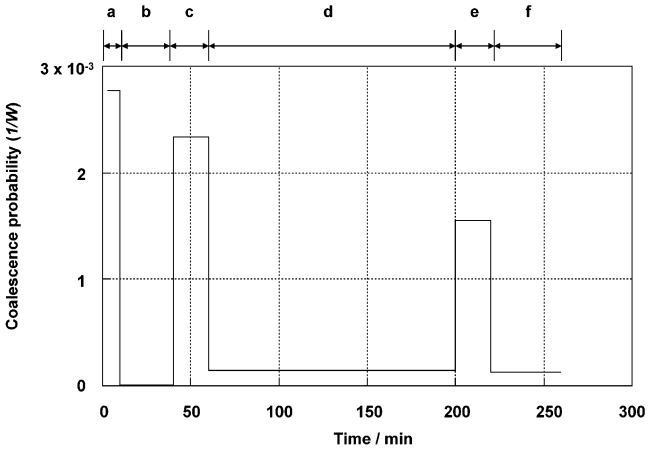

Figure 6. Coalescence probability ($1/W$) (see text) as a function of the elapsed time. In regimes a, c, and e, where the coalescence take places, the probability is sizable, and otherwise almost zero.

In an Ostwald ripening regime, droplets with the radius of a_0 grow into larger ones with the radius of a by the sacrifice of smaller droplets; larger ones become larger, whereas smaller ones become smaller. The ζ-potential (ζ_{ost}) of the growing droplets is expressed as

$$\zeta_{ost} = \zeta_0 a_0^2 \frac{1}{a^2} \tag{7}$$

where ζ_0 is the ζ-potential of a droplet with radius of a_0. The laser Doppler method probably gives the ζ_{ost}-potential in an Ostwald ripening regime because light scattering occurs more significantly by the growing droplets having large volumes than by the diminishing droplets having small volumes. Therefore, the ζ-potential observed by the method, which is approximately equal to the ζ_{ost}-potential, should decrease with the elapsed time because a increases with the elapsed time.

On the other hand, the ζ-potential (ζ_{coales}) of coalesced droplets with the radius of a is expressed in terms of the ζ-potential (ζ_0) of small coalescing droplets with the radius of a_0 as

$$\zeta_{coales} = \frac{\zeta_0}{a_0} a \tag{8}$$

Similarly, the laser Doppler method provides the ζ-potential (ζ_{coales}) of the coalesced droplets because of its higher sensitivity to droplets with larger volumes. It follows that the ζ-potential observed, which is represented by the ζ_{coales}-potential, increases with the elapsed time in the coalescence regime because a increases with the elapsed time. In summary, the ζ-potential observed by the laser Doppler method decreases in an Ostwald ripening regime (see eq 7) while increases in a coalescence regime (see eq 8), if the ζ-potential is determined from the laser Doppler method.

Actually, the ζ-potential observed by the laser Doppler method increases and decreases with the elapsed time as shown in Figure 5. As described above, in the time regimes where the ζ-potential increases with the elapsed time, the droplets grow via coalescence, whereas in the time regimes where the ζ-potential decreases with the elapsed time, the droplets grow

via Ostwald ripening. Thus, the dependence of the ζ-potential on the elapsed time supports the growth mechanism consisting of Ostwald ripening and coalescence. The timings that the Ostwald ripening and the coalescence regimes appear shown in Figure 5 do not agree with those shown in Figure 4 because these two measurements were performed separately. The timings change sensitively with the experimental condition employed.

Summary

As described in this report, we employed a single-droplet detection method for the investigation of the growth mechanism of surfactant-free *n*-decane droplets dispersed in pure water and revealed that Ostwald ripening and coalescence take place alternatively because the droplets loose their surface charge as the Ostwald ripening proceeds and then the droplets coalesce. This method has potential advantages in the studies of emulsions that the individual droplets in the emulsions can be observed without worrying about statistical treatment of the droplets.

Acknowledgment. The authors are indebted to Professors R. N. Zare and D. T. Chiu for the technical advise for the single-molecule detection method. This work was supported by the Cluster Research Project of the Genesis Research Institute, Inc.

References and Notes

(1) Ostwald, W. *Z. Phys. Chem. (Leipzig)* **1900**, *34*, 295.
(2) Taylor, P. *Colloids Surf., A* **1995**, *99*, 175.
(3) Taylor, P. *Adv. Colloid Interface Sci.* **1998**, *75*, 107.
(4) Higuchi, W. I.; Misra, J. *J. Pharm. Sci.* **1962**, *51*, 459.
(5) Thomson, W. *Philos. Mag.* **1871**, *42*, 448.
(6) Lifshitz, I. M.; Slyozov, V. V. *J. Phys. Chem. Solids* **1961**, *19*, 35.
(7) Wagner, C. *Z. Elektochem.* **1961**, *65*, 581.
(8) Derjaguin, B. V.; Landau, L. D. *Acta Physicochim. URSS* **1941**, *14*, 633.
(9) Verwey, E. J. W.; Overbeek, J. Th. G. *Theory of the Stability of Lyophobic Colloids*; Elsevier: Amsterdam, 1948.
(10) Deshikan, S. R.; Papadopoulos, K. D. *J. Colloid Interface Sci.* **1995**, *174*, 302.
(11) Deshikan, S. R.; Papadopoulos, K. D. *J. Colloid Interface Sci.* **1995**, *174*, 313.
(12) Chen, J. D.; Hahn, P. S.; Slattery, J. C. *AIChE J.* **1984**, *30*, 622.
(13) Chen, J. D. *J. Colloid Interface Sci.* **1985**, *107*, 209.
(14) Chen, J. D.; Hahn, P. S.; Slattery, J. C. *AIChE J.* **1988**, *34*, 140.
(15) Weiss, J.; McClements, D. J. *Langmuir* **2000**, *16* (5), 2145.
(16) Kamogawa, K.; Sakai, T.; Momozawa, N.; Shimazaki, M.; Enomura, M.; Sakai, H.; Abe, M. *J. Jpn. Oil Chem. Soc.* **1998**, *47*(2), 159.
(17) Kamogawa, K.; Matsumoto, M.; Kobayashi, T.; Sakai, T.; Sakai, H.; Abe, M. *Langmuir* **1999**, *15* (6), 1913.
(18) Kamogawa, K.; Akatsuka, H.; Matsumoto, M.; Yokoyama, S.; Sakai, T.; Sakai, H.; Abe, M. *Colloids Surf., A* **2001**, *180*, 41.
(19) Sakai, T.; Kamogawa, K.; Harusawa, F.; Momozawa, N.; Sakai, H.; Abe, M. *Langmuir* **2001**, *17* (2), 255.
(20) Sakai, T.; Kamogawa, K.; Nishiyama, K.; Sakai, H.; Abe, M. *Langmuir* **2002**, *18* (6), 1985.
(21) Sakai, T.; Takeda, Y.; Mafuné, F.; Abe, M.; Kondow, T. *J. Phys. Chem. B* **2002**, *106* (19), 5017.
(22) Evens, D. F.; Wennerstrom, H. *The Colloidal Domain*, 2nd ed.; Wiley-VCH: New York, 1999.
(23) Reerink, H.; Overbeek, J. Th. G. *Discuss. Faraday Soc.* **1954**, *18*, 74.
(24) Taylor, A. J.; Wood, F. W. *Trans. Faraday Soc.* **1957**, *53*, 523.
(25) Marinova, K. G.; Alargova, R. G.; Denkov, N. D.; Velev, O. D.; Petsev, D. N.; Ivanov, I. B.; Borwankar, R. P. *Langmuir* **1996**, *12*, 2045.